

Journal of Visualized Experiments

Single-molecule förster resonance energy transfer methods for real time investigation of the resolution of the Holliday junction by GEN1 --Manuscript Draft--

Article Type:	Invited Methods Article - JoVE Produced Video
Manuscript Number:	JoVE60045R2
Full Title:	Single-molecule förster resonance energy transfer methods for real time investigation of the resolution of the Holliday junction by GEN1
Keywords:	Holliday junction single-molecule FRET homologous recombination 5' nucleases Gap endonuclease I (GEN1) Holliday junction resolvases
Corresponding Author:	Samir Hamdan King Abdullah University of Science and Technology Thuwal, Thuwal SAUDI ARABIA
Corresponding Author's Institution:	King Abdullah University of Science and Technology
Corresponding Author E-Mail:	mohamed.sobhy@kaust.edu.sa
Order of Authors:	Mohamed A. Sobhy Amer Bralić Vlad-Stefan Raducanu Muhammad Tehseen Yujing Ouyang Masateru Takahashi Fahad Rashid Manal S. Zaher Samir Hamdan
Additional Information:	
Question	Response
Please indicate whether this article will be Standard Access or Open Access.	Open Access (US\$4,200)
Please indicate the city, state/province, and country where this article will be filmed . Please do not use abbreviations.	Thuwal, Saudi arabia

TITLE:

Single-Molecule Förster Resonance Energy Transfer Methods for Real-Time Investigation of the Holliday Junction Resolution by GEN1

AUTHORS AND AFFILIATIONS:

Mohamed A. Sobhy*, Amer Bralić*, Vlad-Stefan Raducanu, Muhammad Tehseen, Yujing Ouyang, Masateru Takahashi, Fahad Rashid, Manal S. Zaher, Samir M. Hamdan*

Laboratory of DNA Replication and Recombination, Biological and Environmental Sciences and Engineering Division (BESE), King Abdullah University of Science and Technology (KAUST), Thuwal, Saudi Arabia

*These authors contributed equally to this work.

Corresponding Authors:

Samir M. Hamdan (samir.hamdan@kaust.edu.sa)
Mohamed A. Sobhy (mohamed.sobhy@kaust.edu.sa)

Email Addresses of Co-Authors:

Amer Bralić (amer.bralic@kaust.edu.sa)
Vlad-Stefan Raducanu (vladstefan.raducanu@kaust.edu.sa)
Muhammad Tehseen (muhammad.tehseen@kaust.edu.sa)
Yujing Ouyang (yujing.ouyang@kaust.edu.sa)
Masateru Takahashi (masateru.takahashi@kaust.edu.sa)
Fahad Rashid (fahad.rashid@kaust.edu.sa)
Manal Zaher (manal.zaher@kaust.edu.sa)

KEYWORDS:

Holliday junction, single-molecule FRET, homologous recombination, 5' nucleases, gap endonuclease I, GEN1, Holliday junction resolvases

SUMMARY:

Presented here is a protocol for performing single-molecule Förster resonance energy transfer to study HJ resolution. Two-color alternating excitation is used for determining the dissociation constants. Single-color time lapse smFRET is then applied in real-time cleavage assays to obtain the dwell time distribution prior to HJ resolution.

ABSTRACT:

Bulk methods measure the ensemble behavior of molecules, in which individual reaction rates of the underlying steps are averaged throughout the population. Single-molecule Förster resonance energy transfer (smFRET) provides a recording of the conformational changes taking place by individual molecules in real-time. Therefore, smFRET is powerful in measuring structural changes in the enzyme or substrate during binding and catalysis. This work presents a protocol for single-molecule imaging of the interaction of a four-way Holliday junction (HJ) and

gap endonuclease I (GEN1), a cytosolic homologous recombination enzyme. Also presented are single-color and two-color alternating excitation (ALEX) smFRET experimental protocols to follow the resolution of the HJ by GEN1 in real-time. The kinetics of GEN1 dimerization are determined at the HJ, which has been suggested to play a key role in the resolution of the HJ and has remained elusive until now. The techniques described here can be widely applied to obtain valuable mechanistic insights of many enzyme-DNA systems.

INTRODUCTION:

Single-molecule methods based on fluorescence detection provide high signal-to-noise ratios¹. FRET is a spectroscopic technique that can measure distances in the range of 1–10 nm, rendering this technique as a molecular ruler for measuring distances in the nanometer range^{2,3}. The absorption spectrum of the acceptor has a partial spectral overlap with the donor's emission spectrum at the shorter wavelength end. FRET is mediated by the radiationless energy transfer between a donor and acceptor pair, whereas the efficiency of energy transfer is dependent on the distance and orientation of the acceptor⁴.

Several approaches have been implemented to minimize the background and improve the detection efficiency of the fluorescence signal^{5,6}. One approach is confocal microscopy, in which a pinhole restricts the excitation spot to a size below the diffraction limit⁷. Another approach is total internal reflection fluorescence (TIRF), which is a wide-field illumination technique in which the light is directed off-axis above a critical angle⁸. The light is then totally internally reflected at the interface between the glass and aqueous solution, generating an evanescent wave that only illuminates the fluorophores attached to the glass surface and prevents background from the fluorophores in the rest of the solution.

In confocal microscopy, the molecules can be either freely diffusing or surface immobilized. The attained temporal resolution can be within microseconds to several milliseconds⁹. The confocal detection for a single molecule is performed by single-photon avalanche diode (SPAD) and point-by-point scanning of the region of interest¹⁰. In TIRF, a time-series of a few hundreds of molecules immobilized on the surface is recorded by a position-sensitive two-dimensional charge coupled detector (CCD). The CCD amplifies the fluorescence signal either by intensified phosphor screen and microchannel plate or on-chip multiplication of photoelectrons (EMCCD). The temporal resolution is dependent on the readout speed and quantum efficiency of the CCD and usually on the order of few tens of milliseconds⁶.

HJ is a central intermediate in DNA repair and recombination¹¹⁻¹⁴. HJ has two continuous and two crossing strands that connect between the continuous strands without intersecting each other. HJ exists in solution as X-stacked conformers, which undergo continuous isomerization by the continuous strands becoming crossing and the crossing strands becoming continuous in the other conformer¹⁵. Isomer preference of the HJ is dependent on the core sequence and ionic environment and has been extensively studied by FRET¹⁶⁻¹⁹.

GEN1²⁰ is a monomeric protein in solution²¹ and requires dimerization to cleave the HJ, thus

allowing proper separation of the recombined strands^{22,23}. The stacking conformer preference of the HJ influences the outcome of genetic recombination by setting the orientation of the resolution by the HJ resolvases²⁴. Understanding how GEN1 binds the HJ, coordinates the two incisions, and ensures its full resolution have all been under intensive study^{21-23,25-30}.

In this study, an objective based TIRF set-up is used as described previously³¹. Two-color alternating excitation (ALEX) is applied to determine the conformational changes upon the interaction of GEN1 with fluorophore labeled HJ. ALEX produces 2D histograms based on two ratiometric parameters FRET efficiency E , which is donor-acceptor distance-dependent, and the stoichiometry parameter S , which measures the donor-acceptor stoichiometry³². ALEX enables the sorting of fluorescent species based on the stoichiometries of the fluorophores including donor-only, acceptor-only, and mixed subpopulations. ALEX can extend the use of FRET to the full range and can detect differences in fluorophore brightness and oligomerization as well as monitor macromolecule-ligand interactions³³.

It is found that GEN1 consistently succeeds in resolving the HJ within the lifetime of the GEN1-HJ complex. The time-dependent conformational changes are derived from the time-traces of individual molecules, while the histograms represent the distribution of the underlying populations. Using time-lapse single-color FRET, fast on-rates and slow off-rates for the GEN1 dimer are demonstrated, which increase the affinity of the assembled GEN1 dimer at the first incision product.

PROTOCOL:

1. Preparation of surface-functionalized coverslips

1.1 Cleaning

1.1.1. Place five coverslips (24 mm x 60 mm) in ethanol inside a Coplin jar. Sonicate in ethanol then in 1 M potassium hydroxide for 30 min for 3x. Wash in acetone 3x then decant.

1.2 Silanization

1.2.1. Prepare a solution of 2.8% 3-aminopropyltriethoxysilane (APTES) in acetone. Seal the APTES bottle with a paraffin film and store at 4 °C.

NOTE: Use safety goggles and work under a fume hood. The container of the silane solution should be completely dry and rinsed by acetone immediately before and after pouring the silane solution into the jar.

1.2.2. Pour 70 mL of the 2.8% APTES solution into the Coplin jar containing the coverslips. Shake the jar for 4 min in an orbital shaker.

1.2.3. Let the jar stand on the bench for 5 min, sonicate for 1 min, and finally keep the jar on

the bench for another 10 min for the silane to react with the hydroxyl groups on the glass surface.

1.2.4. Quench the reaction by the addition of 1 L of deionized water by pouring water directly into the jar for rapid solvent exchange. Rinse the slides 3x in water by sideways shaking of the jar on a flat surface.

1.2.5. Take the coverslips out of the jar and place them onto an aluminum foil tray. Bake the coverslips in an oven at 110 °C for 30 min to dry the coverslips and cure the silane. Leave the tray on the bench for the coverslips to cool down to room temperature.

1.3 PEGylation

1.3.1. Warm up the biotinylated PEG and PEG, then store at -20 °C to room temperature (RT) to prevent the condensation of moisture upon opening the container.

1.3.2. Place five coverslips with the silanized surface facing up on a box. Place two cover glass slips (22 mm x 22 mm) as spacers along the edges of the silanized coverslips.

1.3.3. Once warmed up, make biotinylated PEG and PEG solutions at a ratio of ~1:100 in 1 mL of fresh, 0.1 M sodium bicarbonate solution by adding 1.5 mg of biotinylated PEG and 150 mg of PEG into a 1.5 mL tube.

1.3.4. Vortex the tube to dissolve PEG and spin down to remove air bubbles.

NOTE: Going forward from this step, be quick, because PEG hydrolyzes in solution within a timescale of min.

1.3.5. Quickly apply 100 µL of the PEG solution to each coverslip. Take another baked coverslip and place its upper silanized surface face-down on top of the coverslip with the PEG solution, hence forming a glass-solution-glass sandwich in which the 22 mm x 22 mm non-silanized coverslips allow the two functionalized coverslips to be separated easily.

1.3.6. Incubate the coverslips overnight (16 h) in the dark and at RT. Once the incubation is complete, take the coverslips apart, then rinse 10x using deionized water by washing from the side with a squirt bottle.

1.3.7. Dry the coverslips under a flow of dry nitrogen. Store the dry coverslips under a vacuum.

NOTE: The slides can be used for 1 month without degradation of quality.

2. Preparation of flow cell

2.1. Single-channel flow cell

2.1.1. Drill two holes with 1.22 mm diameter in the middle part of a quartz slide (50 mm x 20 mm) with the centers situated 37 mm apart and 6.5 mm from the edge of the slide (**Figure 1A**).

2.1.2. Cut out a 41 mm x 2.25 mm channel into a 50 mm x 20 mm piece of a double-adhesive sheet using an electronic cutter.

2.1.3. Peel off the plastic side of the protective cover and align the edges of the piece with the edges of the quartz slide. Remove trapped air bubbles by pressing gently with a pair of polytetrafluoroethylene tweezers.

2.1.4. Peel off the paper side of the adhesive piece. Mount the piece onto the functionalized surface of the coverslip.

2.1.5. Cut polyethylene tubing (I.D. 1.22 mm) into a length of 11 cm for the inlet and 25 cm for the outlet. Insert the tube into the previously drilled holes as inlet and outlet for the flow cell.

2.1.6. Use 5 min epoxy glue to seal around the edges of the quartz-coverslip interface and around the tubes for the inlet and outlet.

2.1.7. Use the flow cell immediately once it dries or store under dry vacuum for later use.

2.1.8. Dissolve avidin in PBS to a concentration of 0.03 mg/mL. Filter through 0.2 μ m syringe filter.

2.1.9. Flow avidin into the flow cell using a 1 mL syringe. Use another syringe filled with buffer to wash out excess avidin. Be careful not to introduce air bubbles while exchanging the syringes.

2.2. Multiple-channel flow cell

2.2.1. Drill six holes with a diameter of 1.22 mm on each of the long sides of a quartz slide (76 mm x 25 mm) (**Figure 1B**). Make the holes 4.5 mm from the edge of the slide and 9.3 mm apart. Ensure the distance between the centers of each hole pair is 15 mm.

2.2.2. Cut out six channels (20 mm x 2.25 mm) into a 76 mm x 25 mm piece of double-adhesive tape using the electronic cutter.

2.2.3. Peel off the plastic side of the protective cover and align the edges of the adhesive piece with the edges of the quartz slide. Remove any trapped air bubbles by gentle pressing using a pair of polytetrafluoroethylene tweezers.

2.2.4. Peel off the paper side of the adhesive piece and mount onto the functionalized surface of the coverslip.

NOTE: Sometimes peeling off the paper side and attaching to the quartz slide works well in the multichannel flow cell.

2.2.5. Cut the inlet tubes (11 cm) and outlet tubes (25 cm) for the six channels. Prepare the flow cell as described in steps 2.1.6–2.1.9.

2.2.6. Connect the outlet of the first channel to the pump. Place the inlet into 0.5 mL tube with OSS.

NOTE: The length of the inlet tube is chosen to maximize the number of events in the cleavage experiments performed under continuous flow by synchronizing time of enzyme entrance into the flow cell and start of imaging thus decreasing premature photobleaching of the fluorophores.

2.2.7. Move to a new channel by disconnecting the outlet of the used channel. Close the outlet with a plug made from a syringe needle sealed with glue in the plastic part. Close the inlet of the used channel.

3. Preparation of oxygen scavenging system (OSS)

3.1. Dissolve 0.2 g of (±)-6-hydroxy-2,5,7,8-tetramethylchromane-2-carboxylic acid (triplet state quencher which minimizes blinking of the fluorophores) in 800 µL of methanol.

3.2. Add 6 mL of deionized H₂O and add 1 N NaOH dropwise until it dissolves. Filter through a syringe filter, make into 1 mL aliquots, and store at -80 °C. The stock concentration is ~100 µM.

3.3. Prepare a fresh solution of 3,4-dihydroxybenzoic acid (PCA) by dissolving 61 mg of PCA powder in 4 mL of ddH₂O. The stock concentration is ~100 nM.

3.4. Add 58 µL of 10 N NaOH dropwise, making sure to vortex after each drop until PCA is fully dissolved (pH = 9).

3.5. Dissolve 5.3 mg of protocatechuate 3,4-dioxygenase (3,4-PCD) in 7 mL of PCD storage buffer (**Table 1**). 3,4-PCD removes oxygen from the binding/cleavage buffers by catalyzing the oxidation of protocatechuic acid³⁴.

3.6. Divide the PCD solution into 1 mL aliquots. The stock concentration is ~1 µM. Snap-freeze the aliquots in liquid nitrogen and store at -80 °C for long-term storage or at -20 °C for short-term storage.

3.7. Prepare a fresh binding buffer (**Table 1**). Substitute 2 mM CaCl₂ with 2 mM MgCl₂ for smFRET cleavage experiments.

3.8. Prepare 1 mL of the imaging buffer (**Table 1**). Keep the imaging buffer on ice until it is introduced into the flow cell to maintain the activity of the oxygen scavenging system.

4. Preparation of fluorescently labeled HJs

4.1. Reconstitute the lyophilized oligos (**Table 2**) in Tris-EDTA buffer (**Table 1**) to a concentration of 100 μ M.

4.2. Prepare the synthetic junction by mixing equimolar portions \sim 3 μ L of each of the X₀ oligos listed in **Table 1**.

4.3. Anneal by heating at 95 °C for 5 min followed by slow cooling to RT at a rate of 1 °C/min. Use either a heat block or PCR thermocycler to achieve the desired cooling rate.

4.4. Load the mixture on 8 cm x 8 cm of 10% Tris-borate-EDTA polyacrylamide gel. Apply 100 V and run the gel for \sim 2 h. The bands are clearly seen by eye, and their color is purple.

4.5. Excise the band of the annealed substrate with a clean blade. Transfer the gel piece into an autoclaved 1.5 mL tube.

4.6. Crush the gel piece inside the tube with a clean plunger then add 100 μ L of TE100 buffer (**Table 1**).

4.7. Extract the HJ by shaking the tube at 20 °C at 1,500 rpm in a thermomixer for \sim 2 h or incubate overnight at 4 °C.

4.8. Perform ethanol precipitation on the solution containing the substrate³⁵.

4.9. Resuspend the substrate in 20 μ L of TE100 buffer (**Table 1**). The final concentration is 1–3 μ M. Aliquot 2 μ L in each tube and store at -20 °C.

5. Protein expression and purification of GEN1

5.1. Construct the plasmid for the expression of truncated human GEN1¹⁻⁵²⁷ with hexa histidine-tag at the C-terminus²⁰ by PCR of the entry vector.

NOTE: N-terminal tagging would result in the inactivation of GEN1. The unstructured C-tail renders the purification of the full length GEN1 significantly harder. Also, the full length GEN1 was reported to exhibit less activity than truncated version²³.

5.2. Transform the expression vector into *E. coli* BL21-CodonPlus (DE3)-RIPL strain.

5.3. Inoculate the transformed cells into two 6 L flasks each containing 2 L of Luria broth media at 37 °C with shaking at 180 rpm until an OD₆₀₀ of 0.8 is reached.

309

310 5.4. Cool down the culture to 16 °C and induce GEN1 expression with 0.1 mM isopropyl-β-d-

311 thiogalactopyranoside (IPTG) for 48 h.

312

313 5.4. Harvest the cells by spinning them down at 4 °C at 1000 x *g* in a centrifuge. Each liter of

314 culture yields 5–6 g of the pellet.

315

316 5.5. Discard the supernatant and resuspend the pelleted cells in lysis buffer (**Table 1**) using 4

317 mL/g of cells.

318

319 5.5. Perform cell lysis using a cell disruptor at 30 kPsi then spin down at 10,000 x *g* for 1 h at

320 4 °C. Collect the supernatant and filter it on ice using 0.45 μm filters.

321

322 5.6. Perform protein purification using FPLC by passing the filtrate through a 5 mL Ni-NTA

323 column at 2.5 ml/min flow rate using Buffer A (**Table 1**).

324

325 5.7. Wash with 15 column volumes (CV). Elute with a linear gradient of Buffer A and 500 mM

326 Imidazole over 20 CV in 5 mL fractions. GEN1 elutes from the column at around 100 mM

327 Imidazole.

328

329 5.8. Pipette 10 μL aliquots from the collected fractions, add equal volume of 2x SDS loading dye

330 to each aliquot. Denature the samples by heating at 90 °C for 5 min, cool, and spin down the

331 samples.

332

333 5.9. Load the samples onto 10% Bis-Tris gel. Run the gel for 30–45 min at 200 V. Stain using

334 Coomassie Brilliant Blue, then destain. Collect the fractions that contain purified GEN1.

335

336 5.10. Reduce the salt concentration of the combined fractions to 100 mM by dilution using

337 buffer C (**Table 1**).

338

339 5.11. Pass the low salt protein through a 5 mL heparin column at a flow rate of 3 mL/min using

340 Buffer B (**Table 1**).

341

342 5.12. Wash with 10 CV. Elute using a gradient of 20 CV with Buffer B and 1 M NaCl. Collect 5 mL

343 fractions in which GEN1 elutes around 360 mM NaCl.

344

345 5.13. Check the eluted fractions for purified GEN1 fractions as described in step 5.8. Combine

346 those fractions and dilute to 100 mM NaCl using Buffer C.

347

348 5.14. Load the lower salt protein onto a cation exchange column at 1 mL/min flow rate using

349 Buffer B.

350

351 5.15. Elute by a gradient of 40 CV using Buffer B and 1 M NaCl. Collect 1.7 mL fractions in which

352 GEN1 elutes around 300 mM NaCl.

353
354 5.16. Check for the purity of GEN1 in the eluted fractions as described in step 5.8.

355
356 5.17. Combine the purest fractions and dialyze at 4 °C against storage buffer (**Table 1**). Perform
357 at least one exchange of the buffer during dialysis.

358
359 5.18. Measure the protein concentration ~0.5–1 mg/mL. Aliquot the dialyzed protein in 10–15
360 µL volumes in small tubes, flash-freeze in liquid nitrogen, and store at -80 °C.

361 362 **6. Single-molecule FRET experiments**

363
364 NOTE: The smFRET experiments are performed on a custom-built objective based TIRF set-up
365 (**Figure 1C**) described previously³¹.

366 367 **6.1 Single-color FRET experiments**

368
369 6.1.1. Apply one drop of immersion oil onto the 100x TIRF objective. Set the EMCCD to suitable
370 gain to optimize the signal to background and prevent saturation.

371
372 NOTE: Do not look directly into the laser beam and wear protective goggles when aligning the
373 laser.

374
375 6.1.2. Place the flow cell carefully on the sample holder. Gradually raise the objective using
376 coarse adjustment until the oil touches the coverslip.

377
378 6.1.3. Turn on the green laser (532 nm). Switch to fine adjustment mode of the objective. Direct
379 the emission to the camera port to observe the image on the monitor.

380
381 6.1.4. Adjust the height of the objective until the functionalized surface of the coverslip is
382 brought in focus and can be observed on the monitor.

383
384 NOTE: The image acquisition by EMCCD triggers the laser excitation via the acousto-optic
385 tunable filter (AOTF) to prevent sample photobleaching when images are not being acquired.

386
387 6.1.5. Check that the background from the functionalized surface of the coverslips does not
388 exceed few spots before flowing in the fluorescently labeled HJ.

389
390 6.1.6. Dilute the stock substrate approximately 1000 times in TE100 buffer (**Table 1**) to a final
391 concentration of 1–5 nM. Pipette 0.2–0.5 µL of the diluted substrate into 120 µL of the imaging
392 buffer with OSS into a 0.5 mL tube.

393
394 6.1.7. Connect the outlet of the flow cell to the syringe pump. Insert the inlet tube of the flow
395 cell into 1.5 mL tube and operate the syringe pump at a flow rate of 30–50 µL/min to withdraw
396 the solution from the tube.

6.1.8. Frequently check the surface for good coverage (100–300 of homogeneously distributed, well-spaced substrate) by imaging briefly with the green laser.

6.1.9. If the surface coverage is still not enough either wait for a few min for the fluorescently labeled HJ from the solution to settle onto the surface or repeat the flowing step.

6.1.10. Flow another 120 μL of imaging buffer (**Table 1**) at 30–50 $\mu\text{L}/\text{min}$ to wash unbound fluorescently labeled HJ. Then let the flow cell sit for 5 min to allow for the OSS to deplete dissolved oxygen. The photobleaching of the fluorophores should be minimal at the start of imaging.

6.1.11. Set the exposure time (~ 60 ms), the cycle time will be automatically set by software based on the speed of data transfer (~ 104 ms), and specify the desired number of cycles or frames (~ 400). The emission from donor (Cy3) and acceptor (Alexa Fluor 647) is split into two color channels by an image splitter device.

6.1.12. Find a suitable area on the surface, focus the image by adjusting the height of the objective and record and save the movie in 16-bit TIFF format.

6.1.13. Move to a new area.

NOTE: Always move in one direction only (i.e., from outlet to inlet) to avoid imaging the same area twice.

6.1.14. Prepare 1, 2, 5, 10, 25, 50, 75, and 100 nM GEN1 in 120 μL of imaging buffer one at a time. Flow the solution at a flow rate of 3050 $\mu\text{L}/\text{min}$.

NOTE: If the required measurement is done under steady state as in the binding of HJ by GEN1 or the isomerization of the free HJ, then wait 3–5 min after the flow stop to record the movie. Acquire three to four movies from new areas for each GEN1 concentration.

6.1.15. If the measurement is performed under continuous flow as in cleavage of HJ by GEN1 then start recording 5–10 s before the entrance of GEN1 into the flow cell. Repeat the measurement by moving to a new channel in the six-channel flow cell.

6.1.16. At the end, use a fixed fluorescent bead slide to map the donor and acceptor particles to each other in the image splitting device.

6.1.17. Add 0.2 μL of 1 μm diameter fluorescent beads into 500 μL of 1 M Tris (pH = 8.0) to allow the beads to stick to the surface.

6.1.18. Cut a square (18 mm x 18 mm) inside a 22 mm x 22 mm piece of a double-sided adhesive seal. Peel off and stick the piece to the middle of a 76 mm x 25 mm quartz slide.

6.1.19. Place 50 μL of the diluted beads solution and leave for 5–10 min to settle. Attach a 22 mm x 22 mm coverslip on top of the square piece. Dry excess beads solution with tissue, then seal the chamber by epoxy glue.

6.1.20. Acquire 100 frames of the beads slide at a 60 ms exposure time.

CAUTION: Lower the laser power and the EMCCD gain to minimum to avoid saturation of the detector.

6.1.21. Install the software package (e.g., TwoTones) and open the movies therein as indicated in the user manual³⁶. Select the positions of the individual beads in the donor and acceptor channels. Generate a transformation matrix as described in the manual.

NOTE: This software uses transformation matrix to match the positions of the particles in the donor and acceptor channels and correct for any slight misalignment in the image splitting device.

6.1.22. Go to **File**, press **Load Movie**, then select the movie file and press **Open**. In file menu, press **Load TFORM** and select the transformation matrix generated from the beads slide. Adjust the threshold for the donor and acceptor channels until no false positives are included.

6.1.23. In the **Channel filter** menu, choose **DD&AA** option to select for particles labeled with both donor and acceptor. Check the **Nearest neighbor limit field** to exclude molecules that are very near to each other. Check **Max ellipticity** to exclude very eccentric molecules and check **Width** limits to exclude very broad or very narrow molecules.

6.1.24. Type **plotHistCW** as instructed in **Twotones** manual to construct histograms.

NOTE: The “apparent” FRET efficiency is calculated by the program by dividing the emission of the acceptor by the total emissions from the donor and the acceptor. Twotones uses 100 intervals to bin the distribution of the states of the molecules against the FRET efficiency.

6.1.25. Type **plotTimetraceCW** as instructed in Twotones manual to generate the time-traces for each molecule.

NOTE: Time-traces can be further analyzed by vbFRET³⁷ to identify different FRET states, their respective dwell times, and transition rates between different states.

6.2 Two-color alternating excitation FRET (ALEX) experiments

6.2.1. Record a movie composed of consecutive frames of donor and acceptor emissions by direct excitations with the green and red lasers, respectively, each ~80 ms in duration.

6.2.2. Open the acquired ALEX movies in Twotones. Set the suitable detection threshold as ~300 for the three channels: donor emission due to donor excitation (DexDem); acceptor emission due to donor excitation (DexAem); and acceptor emission due to the direct excitation (AexAem).

6.2.3. Apply the Channel filter DexDem&&DexAem&&AexAem to select for the particles that have both donors and acceptors. Link the particles ~200–300 in the three channels.

6.2.4. Use the plotHistALEX MATLAB code to generate ALEX histograms. Fit different peaks in the histograms to gaussian functions and determine the percentage of each population the area under the curve using Origin software³⁸.

NOTE: The peaks in the binding assay correspond to the bound GEN1-HJ complex, while in the free HJ, the peaks represent the interchanging isomers.

6.2.5. Use the **plotTimetraceALEX** MATLAB code to generate a time-trace for each molecule showing donor emission by direct excitation, and acceptor emissions due to FRET and direct excitation.

NOTE: ALEX time-traces independently to show the emissions of both the donor and acceptor, but at lower temporal resolution than single-color FRET. Similar to single-color FRET, ALEX time-traces can be further analyzed by vbFRET to identify different FRET states and their respective dwell times.

6.2.6. Determine the dissociation constant by fitting the percentages of the bound population versus GEN1 concentration to a hyperbolic function.

6.3 Time lapse single-color FRET

6.3.1. Set the exposure time of the green laser to 60 ms and cycle time to 624 ms or lower, depending on the speed of the observed dynamics.

6.3.2. Set the flow rate to 110 $\mu\text{L}/\text{min}$ in one of channels in the six-channel flow cell. Start the recording briefly before the entrance of GEN1 inside the flow cell.

NOTE: Continuous flow leads to rapid photobleaching of the fluorophores, therefore synchronizing the start of imaging and protein entry maximizes the number of captured events. The optimal syringe pump reading depends on the dead-volume and the exact tubing used to assemble the flow cell; in our case it is ~25 μL .

6.3.3. Acquire a movie of ~125 frames for a total acquisition time of 78 s. At the end of the recording, expose the sample to the red laser for 50 frames each with 25 ms exposure time to probe the acceptor.

NOTE: This method prolongs the observation window in cleavage experiment through decreasing the number of excitation cycles. Kinetic parameters as k_{on} and k_{off} of dimerization are derived by fitting the distribution to a bi-exponential model^{30,38}.

7. Electrophoretic mobility shift assays (EMSA)

7.1. In 50 μ L total volume, incubate the desired concentration of GEN1 with 50 pM Cy5-labeled HJ at RT for 30 min in EMSA binding buffer (Table 1).

7.2. Load the samples on 8 cm x 8 cm of 6% Tris-borate-EDTA gel. Run the gel using 100 V for 1 h + 20 min in 1x TBE buffer at RT.

7.3. Determine the percentage of bound substrate at a GEN1 concentration from its relative contribution to the total fluorescence intensity of the respective lane.

NOTE: GEN1 monomer-HJ (band I) is identified by the agreement of its size with the picomolar binding of GEN1 monomer to the nicked HJ^{21,30}. GEN1-dimer-HJ is assigned to band II because of the stepwise binding of GEN1 monomer to the HJ^{21,23}.

7.4. Calculate the apparent binding constants $K_{d\text{-monomer-app-EMSA}}$ and $K_{d\text{-dimer-app-EMSA}}$ using the equation:

$$Y = \text{Max} \cdot [\text{GEN1}]^n / (K_{d\text{-app-EMSA}}^n + [\text{GEN1}]^n)$$

Where: *Max* is the concentration at which the respective species reached its maximum binding (monomer or dimer); *n* is the Hill coefficient; $K_{d\text{-app-EMSA}}$ is the apparent binding constant of the respective species, denoting the concentration of GEN1 at which half-maximum of monomer or dimer is present.

REPRESENTATIVE RESULTS:

Conformer bias and isomerization of the HJ

The isomerization of HJ has been extensively investigated by FRET through the labeling of two adjacent arms of the junction^{17,18,39}. The donor (Cy3) and acceptor (Alexa Fluor 647) are positioned at the two neighboring arms, R (strand 2) and X (strand 3), respectively (Figure 2A). The stacked-X isomers were assigned by their two continuous strands [i.e., Iso(1,3) or Iso(2,4)]. The ALEX FRET histogram of adjacent-label X_0 shows two peaks that correspond to interchanging of the more abundant Iso(1,3) ($E \sim 0.75$) and less abundant Iso(2,4) ($E \sim 0.40$) (Figure 2B).

Single-color FRET is used to acquire time-traces for recording the rapid conformational changes in the free HJ with high temporal resolution ~ 10 ms via reducing the used area of the EMCCD2 camera. A representative single-color FRET time-trace of X_0 junction shows the transitions between high and low FRET isomers (Figure 2B). The isomerization rates $k_{\text{Iso}(1,3) \rightarrow \text{Iso}(2,4)}$ and

$k_{Iso(2,4)-Iso(1,3)}$ obtained from the dwell time histograms of Iso(1,3) and Iso(2,4) (**Figure 2C**) are consistent with those reported previously¹⁷.

SMFRET demonstrates active distortion of the HJ by GEN1

HJ undergoes structural rearrangement upon binding to GEN1²². Thus, the spacing between the donor and acceptor is similar in both Iso(1,3) and Iso(2,4) (**Figure 3A**). The smFRET binding assays were carried out in the presence of Ca^{2+} to prevent cleavage of the HJ. FRET histograms of the adjacent-label X_0 junction at different GEN1 concentrations were acquired by ALEX (**Figure 3B**). The histogram is fit to two Gaussian functions: one corresponding to the free high FRET Iso(1,3), and the other corresponding to the bound GEN1-HJ population after subtracting the contribution of the Iso(2,4) from the low FRET peak.

At saturating GEN1 concentration, the FRET histogram of X_0 has only a single low FRET peak corresponding to GEN1 bound to either isomer of the HJ as predicted by the model²². The apparent monomer dissociation constant ($K_{d-monomer-app}$) is determined from the hyperbolic fit of the percentages of GEN1-bound population as a function of GEN1 concentration (**Figure 3C**). The adjacent-label nk- X_0 represents a singly nicked version HJ that mimics the product after the first incision reaction. Due to the relief of stacking strain by the simulated nick, nk- X_0 is a non-isomerizing structure⁴⁰ as evident from the single substrate peak at $E \sim 0.40$, unlike X_0 (**Figure 3D** vs. **Figure 3B**). The structure of GEN1-nk- X_0 complex is similar to that of the GEN1- X_0 complex, as indicated by the similarity in FRET efficiencies ($E \sim 0.25$ for nk- X_0 and 0.32 for X_0) (**Figure 3D** vs. **Figure 3B**). The strong binding of GEN1 monomer to nk- X_0 is demonstrated by the 40-fold lower $K_{d-monomer-app}$ value than that of X_0 (**Figure 3E** vs. **Figure 3C**). This tight binding may act as a safeguard mechanism against the incomplete resolution of the HJ in the unlikely event of the dissociation of GEN1 dimer or one of its monomers.

Stepwise binding of GEN1 monomer to the HJ

The binding of GEN1 monomer to the HJ followed by dimer formation is a unique feature for the eukaryotic HJ resolvase GEN1 compared to prokaryotic resolvases, which exist in dimeric form in solution^{21,23,41}. EMSA of GEN1 at 50 pM X_0 shows the stepwise association of GEN1 into higher order complexes, as indicated by the roman numerals in the upper panel (**Figure 4A**). The dissociation constant of GEN1 monomer determined by EMSA ($K_{d-monomer-EMSA}$) coincides with the dissociation constant from the smFRET binding assay $K_{d-monomer-app}$ (**Figure 4A** and **Figure 3C**, respectively). The quantification of band II is used to calculate the equilibrium dissociation constant of GEN1 dimer ($K_{d-dimer-EMSA}$). EMSA of GEN1 at 50 pM nk- X_0 demonstrates the prominent monomer binding as indicated by the very low $K_{d-monomer-app-EMSA}$ which is 30-fold lower than that of X_0 , while its $K_{d-dimer-EMSA}$ is comparable to that of X_0 (**Figure 4B**).

Further evidence that GEN1 monomer binds and distorts the HJ is the observation of a significant number of traces of uncleaved particles with stable low FRET state (**Figure 4C**) in the presence of Mg^{2+} at low GEN1 concentrations. The number of these traces decreased upon increasing GEN1 concentrations. The resolution of the HJ is driven by the tight binding of GEN1 monomer, which supports dimer formation. The monomer binding is observed in the time-traces of the uncleaved nk- X_0 in Mg^{2+} , which extends until few nanomolar concentration (**Figure**

4D). The GEN1 monomer binds tightly to safeguard nk- X_0 , eventually ensuring full resolution through dimer formation.

SMFRET resolution assay of the HJ

The term “cleavage” in smFRET assays is used interchangeably with “resolution” of the HJ, since in this assay only the product release that follows the second cleavage event is detected. The events are recorded by time-lapse single-color excitation to minimize photobleaching of the photo-sensitive acceptor over the acquisition time of ~1.3 min.

The schematic in **Figure 5A** illustrates the incisions of strands 1 and 3 of X_0 Iso(1,3) after the binding and distortion by GEN1 of an X_0 attached to the functionalized glass. Both donor and acceptor go into solution resulting in the loss of their signals after the HJ resolution. The first and second incisions are decoupled in nk- X_0 , which exemplifies a prototype for the partially resolved HJ. Upon binding of GEN1, nk- X_0 adopts a similar structure to X_0 . The resolution proceeds by a single incision in strand 3, as illustrated in **Figure 5B**.

The simultaneous departure of the donor and acceptor after a stable low FRET state in traces of resolved X_0 occurred without the emergence of an intermediate FRET ($E = \sim 0.40$) indicates that complete resolution occurs within the lifetime of the GEN1-HJ complex (**Figure 5C**). Therefore, these results suggest that the HJ resolution occurs within the GEN1-HJ complex lifetime. The resolution of nk- X_0 also proceeds after structural rearrangement and concludes by the departure of the duplex carrying two fluorophores (**Figure 5D**) similar to X_0 .

Kinetics of GEN1 dimerization on GEN1 monomer bound HJ

Time-lapse smFRET measures $\tau_{before-cleavage}$ which mainly includes the time required for dimer formation and resolution of the HJ after the distortion by GEN1 monomer. Applying this technique, direct evidence is provided to support the claim that dimer formation is required for the resolution of both X_0 and nk- X_0 , since the distribution of $\tau_{before-cleavage}$ is GEN1 concentration-dependent.

The apparent rate of the HJ resolution (k_{app}) is defined as the inverse of the mean of $\tau_{before-cleavage}$ at the respective GEN1 concentration. The term “apparent” is used to describe the rate of the HJ resolution, since the possibility that GEN1 remains bound to the product after the HJ resolution cannot be excluded.

The probability density functions (PDF) of the $\tau_{before-cleavage}$ distributions of X_0 (**Figure 6A**) reflect the time for dimer formation, which is longer at low GEN1 concentrations, then shorter at higher GEN1 concentrations. The association and dissociation rates for the dimer, $k_{on-dimer}$ and $k_{off-dimer}$, respectively, are determined from a bi-exponential model³⁰. Similar to, PDFs of nk- X_0 (**Figure 6B**) show a similar distribution to X_0 indicating the requirement for dimer formation.

The plot of k_{app} versus GEN1 concentration was fitted to a hyperbolic function. The apparent catalysis rate constants ($k_{Max-app}$) of X_0 and nk- X_0 are $0.107 \pm 0.011 \text{ s}^{-1}$ and $0.231 \pm 0.036 \text{ s}^{-1}$,

respectively (**Figure 6C**). The plots of k_{app} for X_0 and $nk-X_0$ junctions intersect at GEN1 concentration ~ 5.6 nM because of the faster $k_{Max-app}$ and slower $k_{on-dimer}$ of the nicked compared to the intact junction.

In summary, the relatively fast $k_{on-dimer}$ and slow $k_{off-dimer}$ lead to the progression of the forward reaction towards HJ resolution once the dimer is formed. The strong binding of GEN1 monomer to the $nk-X_0$ junction constitutes a fail-safe mechanism against any unlikely aborted second cleavage or helps to pick up any incompletely unresolved HJs left behind by primary resolution pathways in the cell.

FIGURE LEGENDS:

Figure 1: Single and multiple-channel flow cells and layout of the optical set-up. (A) Schematic of the single-channel flow cell. (B) Schematic of the six-channel flow cell. (C) Layout of the optical set-up depicting the excitation sources, TIRF objective, dichroic mirror installed inside the filter cube, and emission filters used in the image splitter device.

Figure 2: Conformer bias and isomerization of the HJ observed by FRET. (A) Isomerization of the adjacent-label X-stacked HJ conformers named after the two continuous strands. The strands are numbered, while the arms are denoted by letters. The incision sites are shown by arrows. The positions of the donor (green) and acceptor (red) and the change in FRET upon isomerization are indicated. (B) Right panel: FRET time-trace (black) and idealized FRET trace (red) of X_0 at 50 mM Mg^{2+} . Left panel: FRET histogram of X_0 at 50 mM Mg^{2+} . The fluorescence intensities of the donor (green) and acceptor (red) are shown below. (C) The dwell time histograms of adjacent-label X_0 Iso(1,3) and Iso(2,4) were fitted to single-exponential functions to determine the isomerization rates. The uncertainties indicate the 95% confidence interval of the fit. This figure has been modified from previously published literature³⁰.

Figure 3: Active distortion of the HJ by GEN1. (A) Structural modification of adjacent-label HJ based on the proposed model²². (B) ALEX FRET histogram of adjacent-label X_0 has a major high FRET peak ($E = \sim 0.6$) corresponding to Iso(1,3) and lower FRET peak ($E = \sim 0.4$) for Iso(2,4). The entire histogram is fit to two Gaussian functions: one corresponding to the free high FRET Iso(1,3), and the other corresponding to the bound population minus the initial contribution of Iso(2,4) to the total population. (C) The apparent monomer dissociation constant ($K_{d-monomer-app}$) is determined from a hyperbolic fit of the percentages of GEN1-bound populations as a function of GEN1 concentration. (D) FRET histograms of the adjacent-label $nk-X_0$ at different GEN1 concentrations. The area under the low FRET ($E = \sim 0.25$) Gaussian corresponds to the percentage of the bound population. (E) The $K_{d-monomer-app}$ of $nk-X_0$ is determined from the hyperbolic fit of GEN1-bound population. The error bars represent the standard deviations from two or more experiments. This figure has been modified from previously published literature³⁰.

Figure 4: Stepwise binding of GEN1 to the HJ. (A) Electrophoretic mobility shift assay (EMSA) of GEN1 at 50 pM X_0 . Upper panel: the roman numerals indicate the number of GEN1 monomers in the complex. Lower panel: binding of GEN1 monomer to X_0 . The apparent dissociation

constants were obtained from a sigmoidal fit of the respective species and represent the average of two experiments. **(B)** EMSA of GEN1 at 50 pM nk-X₀ demonstrates the prominent monomer binding as indicated by the very low $K_{d\text{-monomer-app-EMSA}}$. **(C)** FRET time-trace of bound but uncleaved adjacent-label X₀ in Mg²⁺. Donor excitation for ~1.3 min was performed, followed by direct acceptor excitation (shaded pink region). **(D)** FRET time-trace of bound but uncleaved adjacent-label nk-X₀ in Mg²⁺. This figure has been modified from previously published literature³⁰.

Figure 5: SMFRET resolution assay of the HJ. **(A)** Schematic of the adjacent-label X₀ Iso(1,3) after distortion by GEN1. The substrate is attached to the functionalized surface via biotin/avidin linkage. The dissociation of GEN1 after the two incisions results in the loss of both donor and acceptor that go into solution. **(B)** Schematic of the resolution of adjacent-label nk-X₀ by cleaving strand 1. **(C)** Time-trace (black) at 2 mM Mg²⁺ of the cleavage of Iso(1,3). The onset of GEN1 binding forms a stable low FRET state until the FRET signal is abruptly lost due to cleavage. Correspondingly, the increase in the donor and the decrease of acceptor fluorescence intensities upon GEN1 binding is followed by the simultaneous disappearance of the fluorescence from both dyes upon cleavage. **(D)** Similarly, the time-trace of nk-X₀ shows a stable low FRET state upon GEN1 binding which is concluded by the abrupt loss of the FRET signal. This figure has been modified from previously published literature³⁰.

Figure 6: Kinetics of GEN1 dimerization on GEN1 monomer bound HJ. **(A)** The probability density function (PDF) plot of the $\tau_{\text{before-cleavage}}$ distribution of X₀ illustrates its dependence on GEN1 concentration. Dwell times of the low FRET state ($\tau_{\text{before-cleavage}}$) at the respective GEN1 concentration were obtained from two or more experiments and used to obtain average rates (k_{app}). The listed k_{app} rates are determined from the inverse of the mean $\tau_{\text{before-cleavage}}$ at the respective GEN1 concentration. The association ($k_{on-dimer}$) and dissociation ($k_{off-dimer}$) rates for dimer formation are calculated from a bi-exponential model³⁸. The errors represent SEM of k_{app} . **(B)** The PDF plot of the $\tau_{\text{before-cleavage}}$ distributions of nk-X₀ and the respective k_{app} rates. **(C)** Plot of k_{app} versus GEN1 concentration fitted to a hyperbolic function to determine the apparent catalytic rate ($k_{Max-app}$). The plot of k_{app} for X₀ and nk-X₀ illustrates the faster initial k_{app} of X₀ which is then surpassed by nk-X₀ above [GEN1] ~5.6 nM. This figure has been modified from previously published literature³⁰.

Table 1: The list of buffers and their compositions used in this study.

Table 2: SMFRET and EMSA HJ substrates. The list of oligonucleotides used for the preparation of the fluorescently labeled HJs for smFRET and EMSA. The oligos were commercially obtained. The fluorescently labeled oligos were HPLC-purified and, when possible, oligos of ≥60 bp were PAGE-purified.

DISCUSSION:

In this study, implemented different smFRET techniques were used to determine the kinetics of

HJ resolution by GEN1³⁰. Similar smFRET approaches were used to follow the double-flap DNA conformational requirement and cleavage by the DNA replication and repair flap endonuclease 1⁴²⁻⁴⁴. Here, critical steps in this protocol are discussed. The silanization reaction should be free from any trace of humidity. The pegylation solution should be applied rapidly to the silanized glass once PEG is dissolved to avoid hydrolysis. In the multi-channel flow cell, any trapped air in the adhesive sheet should be removed to avoid leakage between neighboring channels. The PCA solution should be freshly prepared since it oxidizes over time. The addition of 10 N NaOH should be dropwise, with vortexing in between. The fluorescence background in the coverslip should be minimal before flowing the fluorescently labeled HJ. The imaging in the flow cell should be performed in one direction to avoid imaging bleached areas. In ALEX experiments, the power of the red laser should be reduced to avoid rapid bleaching of the acceptor. In the time-lapse experiments, the cycle time has to be shorter than the fastest event.

smFRET is a sensitive technique that can provide valuable real-time insights in biomolecular reactions. However, this method has several technical challenges, among which is achieving measurable change in FRET during the biochemical reaction. This is necessary to obtain well-separated features in the histograms and distinguishable states in the time-traces. In many cases, smFRET requires careful design of the substrates, selection of the fluorophore pairs and their positions, and amplification of FRET changes in the DNA substrate because of the little structural changes in the substrate⁴⁵. Another approach for performing FRET is to use labeled proteins⁴⁶. The observation window in FRET is limited by the stability of the acceptor such as Cy5 or Alexa Fluor 647 which tend to bleach more rapidly than the donor (Cy3 in this case). Therefore, FRET requires a continuous search for stable fluorophores to extend the experiment duration and efforts to develop oxygen scavenging systems to prolong the fluorescence signal and maximize the signal-to-noise ratio^{47,48}.

Among the tips for troubleshooting in smFRET is balancing the several parameters involved in imaging such as the laser power, exposure time, cycle time, and number of cycles to maximize the fluorescence emission, prolong the experiment duration, and achieve appropriate sampling intervals for the enzyme dynamics. Longer observation times and minimal effects from photobleaching are essential to obtain high fidelity dwell time distributions that represent the enzyme dynamics. ALEX generates better histograms since this method is subjected to lower contributions from photobleached particles compared to single-color FRET. However, the temporal resolution in ALEX is lower than that in single-color FRET.

Finally, smFRET's emphasis on detecting conformational/structural changes in individual molecules in real-time bridges the gap between high resolution structural techniques (i.e., X-ray crystallography, nuclear magnetic resonance, electron microscopy), which provides atomic resolution structural details under static conditions and bulk methods that yield the ensemble average of a measurable property. In many aspects, smFRET has proven to be a powerful technique for studying biological systems in real-time.

DISCLOSURES:

The authors declare no competing financial interests.

ACKNOWLEDGMENTS:

This work was supported by King Abdullah University of Science and Technology through core funding and Competitive Research Award (CRG3) to S. M. H.

REFERENCES:

- 1 Moerner, W. E., Fromm, D. P. Methods of single-molecule fluorescence spectroscopy and microscopy. *Review of Scientific Instruments*. **74** (8), 3597-3619 (2003).
- 2 Ha, T. Single-molecule fluorescence resonance energy transfer. *Methods*. **25** (1), 78-86 (2001).
- 3 Weiss, S. Fluorescence spectroscopy of single biomolecules. *Science*. **283** (5408), 1676-1683 (1999).
- 4 Stryer, L. Fluorescence energy transfer as a spectroscopic ruler. *Annual Review of Biochemistry*. **47**, 819-846 (1978).
- 5 Roy, R., Hohng, S., Ha, T. A practical guide to single-molecule FRET. *Nature Methods*. **5** (6), 507-516 (2008).
- 6 Walter, N. G., Huang, C. Y., Manzo, A. J., Sobhy, M. A. Do-it-yourself guide: how to use the modern single-molecule toolkit. *Nature Methods*. **5** (6), 475-489 (2008).
- 7 Conchello, J. A., Lichtman, J. W. Optical sectioning microscopy. *Nature Methods*. **2** (12), 920-931 (2005).
- 8 Axelrod, D. Total internal reflection fluorescence microscopy in cell biology. *Methods in Enzymology*. **361**, 1-33 (2003).
- 9 Kim, H. D. et al. Mg²⁺-dependent conformational change of RNA studied by fluorescence correlation and FRET on immobilized single molecules. *Proceedings of the National Academy of Sciences of the United States of America*. **99** (7), 4284-4289 (2002).
- 10 Lee, T. H. et al. Measuring the folding transition time of single RNA molecules. *Biophysical Journal*. **92** (9), 3275-3283 (2007).
- 11 Holliday, R. Mechanism for Gene Conversion in Fungi. *Genetical Research*. **5** (2), 282-304 (1964).
- 12 West, S. C. et al. The Formation and Resolution of Holliday Junctions during the Recombinational Repair of DNA Damages. *Journal of Cellular Biochemistry*. 269-269, (1995).
- 13 Cox, M. M. et al. The importance of repairing stalled replication forks. *Nature*. **404** (6773), 37-41 (2000).
- 14 West, S. C. Molecular views of recombination proteins and their control. *Nature Reviews: Molecular Cell Biology*. **4** (6), 435-445 (2003).
- 15 Duckett, D. R. et al. The structure of the Holliday junction, and its resolution. *Cell*. **55** (1), 79-89 (1988).
- 16 Clegg, R. M. et al. Fluorescence resonance energy transfer analysis of the structure of the four-way DNA junction. *Biochemistry*. **31** (20), 4846-4856 (1992).
- 17 McKinney, S. A., Declais, A. C., Lilley, D. M., Ha, T. Structural dynamics of individual Holliday junctions. *Nature Structural Biology*. **10** (2), 93-97 (2003).

833 18 Joo, C., McKinney, S. A., Lilley, D. M., Ha, T. Exploring rare conformational species and
834 ionic effects in DNA Holliday junctions using single-molecule spectroscopy. *Journal of*
835 *Molecular Biology*. **341** (3), 739-751 (2004).

836 19 Hyeon, C., Lee, J., Yoon, J., Hohng, S., Thirumalai, D. Hidden complexity in the
837 isomerization dynamics of Holliday junctions. *Nature Chemistry*. **4** (11), 907-914 (2012).

838 20 Ip, S. C. et al. Identification of Holliday junction resolvases from humans and yeast.
839 *Nature*. **456** (7220), 357-361 (2008).

840 21 Rass, U. et al. Mechanism of Holliday junction resolution by the human GEN1 protein.
841 *Genes & Development*. **24** (14), 1559-1569 (2010).

842 22 Liu, Y. et al. Crystal Structure of a Eukaryotic GEN1 Resolving Enzyme Bound to DNA. *Cell*
843 *Reports*. **13** (11), 2565-2575 (2015).

844 23 Chan, Y. W., West, S. GEN1 promotes Holliday junction resolution by a coordinated nick
845 and counter-nick mechanism. *Nucleic Acids Research*. **43** (22), 10882-10892 (2015).

846 24 van Gool, A. J., Hajibagheri, N. M., Stasiak, A., West, S. C. Assembly of the Escherichia
847 coli RuvABC resolvosome directs the orientation of holliday junction resolution. *Genes &*
848 *Development*. **13** (14), 1861-1870 (1999).

849 25 Lee, S. H. et al. Human Holliday junction resolvase GEN1 uses a chromodomain for
850 efficient DNA recognition and cleavage. *eLife*. **4**, (2015).

851 26 Chan, Y. W., West, S. C. Spatial control of the GEN1 Holliday junction resolvase ensures
852 genome stability. *Nature Communications*. **5**, 4844 (2014).

853 27 Liu, Y., Freeman, A. D., Declais, A. C., Lilley, D. M. J. A monovalent ion in the DNA binding
854 interface of the eukaryotic junction-resolving enzyme GEN1. *Nucleic Acids Research*. **46**
855 (20), 11089-11098 (2018).

856 28 Zhou, R. et al. Junction resolving enzymes use multivalency to keep the Holliday junction
857 dynamic. *Nature Chemical Biology*. **15** (3), 269-275 (2019).

858 29 Bellendir, S. P. et al. Substrate preference of Gen endonucleases highlights the
859 importance of branched structures as DNA damage repair intermediates. *Nucleic Acids*
860 *Research*. **45** (9), 5333-5348 (2017).

861 30 Sobhy, M. A. et al. Resolution of the Holliday junction recombination intermediate by
862 human GEN1 at the single-molecule level. *Nucleic Acids Research*. **47** (4), 1935-1949
863 (2019).

864 31 Sobhy, M. A. et al. Versatile single-molecule multi-color excitation and detection
865 fluorescence set-up for studying biomolecular dynamics. *Review of Scientific*
866 *Instruments*. **82** (11), 113702 (2011).

867 32 Kapanidis, A. N. et al. Fluorescence-aided molecule sorting: analysis of structure and
868 interactions by alternating-laser excitation of single molecules. *Proceedings of the*
869 *National Academy of Sciences of the United States of America*. **101** (24), 8936-8941
870 (2004).

871 33 Lee, N. K. et al. Accurate FRET measurements within single diffusing biomolecules using
872 alternating-laser excitation. *Biophysical Journal*. **88** (4), 2939-2953 (2005).

873 34 Rashid, F. et al. Initial state of DNA-Dye complex sets the stage for protein induced
874 fluorescence modulation. *Nature Communications*. **10** (1), 2104 (2019).

875 35 Sambrook, J., Russell, D. W. Standard ethanol precipitation of DNA in microcentrifuge
876 tubes. *Cold Spring Harbor Protocols*. **2006** (1), doi:10.1101/pdb.prot093377 (2006).

877 36 Holden, S. J. et al. Defining the limits of single-molecule FRET resolution in TIRF
878 microscopy. *Biophysical Journal*. **99** (9), 3102-3111 (2010).

879 37 Bronson, J. E., Fei, J., Hofman, J. M., Gonzalez, R. L., Jr., Wiggins, C. H. Learning rates and
880 states from biophysical time series: a Bayesian approach to model selection and single-
881 molecule FRET data. *Biophysical Journal*. **97** (12), 3196-3205 (2009).

882 38 Kou, S. C., Cherayil, B. J., Min, W., English, B. P., Xie, X. S. Single-molecule Michaelis-
883 Menten equations. *Journal of Physical Chemistry B*. **109** (41), 19068-19081 (2005).

884 39 Clegg, R. M., Murchie, A. I., Lilley, D. M. The solution structure of the four-way DNA
885 junction at low-salt conditions: a fluorescence resonance energy transfer analysis.
886 *Biophysical Journal*. **66** (1), 99-109 (1994).

887 40 Pohler, J. R., Duckett, D. R., Lilley, D. M. Structure of four-way DNA junctions containing
888 a nick in one strand. *Journal of Molecular Biology*. **238** (1), 62-74 (1994).

889 41 Fogg, J. M., Lilley, D. M. Ensuring productive resolution by the junction-resolving enzyme
890 RuvC: large enhancement of the second-strand cleavage rate. *Biochemistry*. **39** (51),
891 16125-16134 (2000).

892 42 Sobhy, M. A., Joudeh, L. I., Huang, X., Takahashi, M., Hamdan, S. M. Sequential and
893 multistep substrate interrogation provides the scaffold for specificity in human flap
894 endonuclease 1. *Cell Reports*. **3** (6), 1785-1794 (2013).

895 43 Rashid, F. et al. Single-molecule FRET unveils induced-fit mechanism for substrate
896 selectivity in flap endonuclease 1. *eLife*. **6**, (2017).

897 44 Zaher, M. S. et al. Missed cleavage opportunities by FEN1 lead to Okazaki fragment
898 maturation via the long-flap pathway. *Nucleic Acids Research*. **46** (6), 2956-2974 (2018).

899 45 Didenko, V. V. DNA probes using fluorescence resonance energy transfer (FRET): designs
900 and applications. *BioTechniques*. **31** (5), 1106-1116, 1118, 1120-1101 (2001).

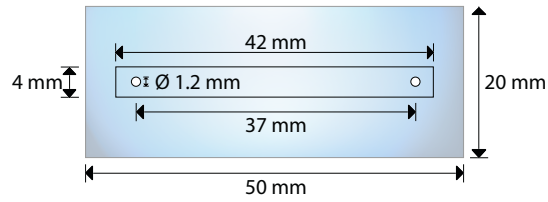
901 46 Toseland, C. P. Fluorescent labeling and modification of proteins. *Journal of Chemical*
902 *Biology*. **6** (3), 85-95 (2013).

903 47 Aitken, C. E., Marshall, R. A., Puglisi, J. D. An oxygen scavenging system for improvement
904 of dye stability in single-molecule fluorescence experiments. *Biophysical Journal*. **94** (5),
905 1826-1835 (2008).

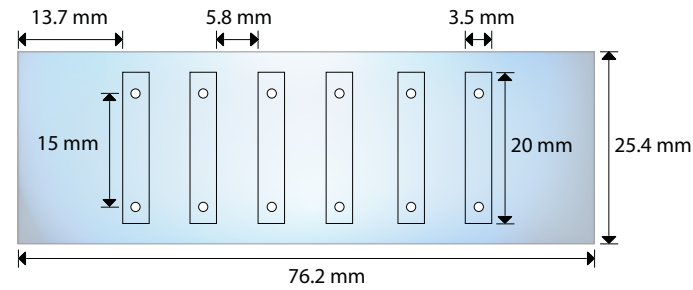
906 48 Swoboda, M. et al. Enzymatic oxygen scavenging for photostability without pH drop in
907 single-molecule experiments. *ACS Nano*. **6** (7), 6364-6369,(2012).

908

A



B



C

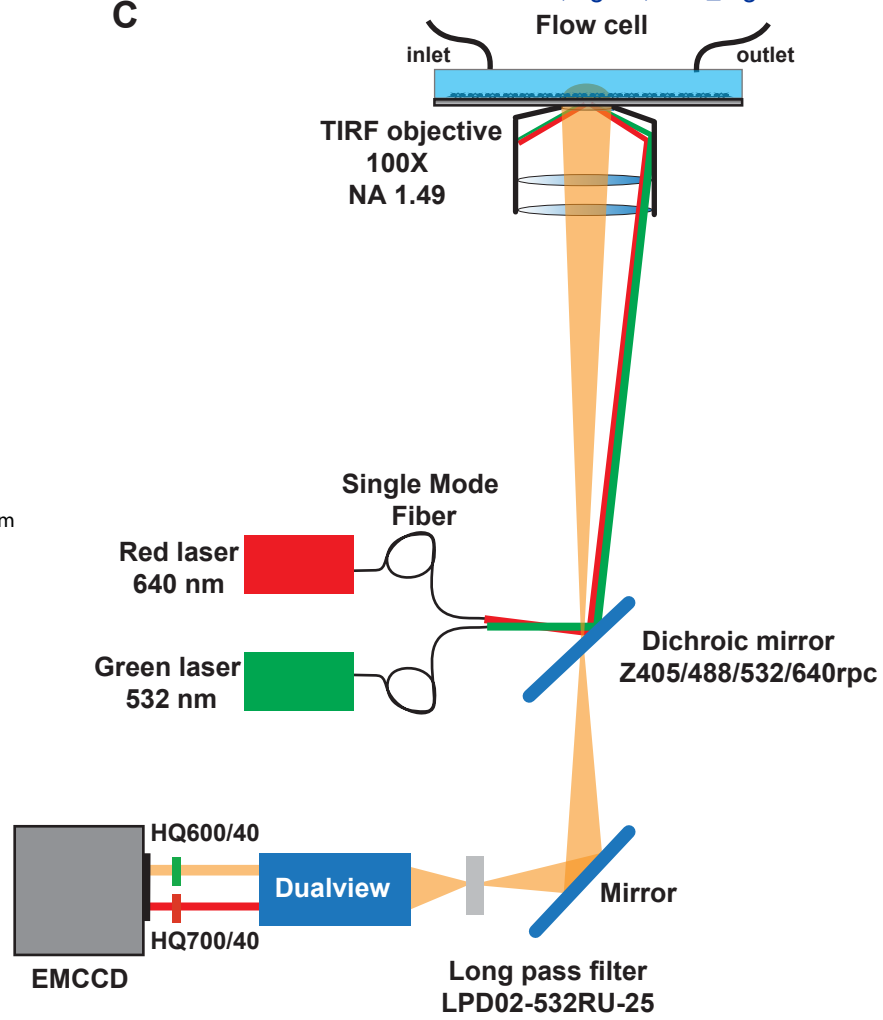


Figure 1 Single and multiple-channel flow cell and layout of the optical setup.

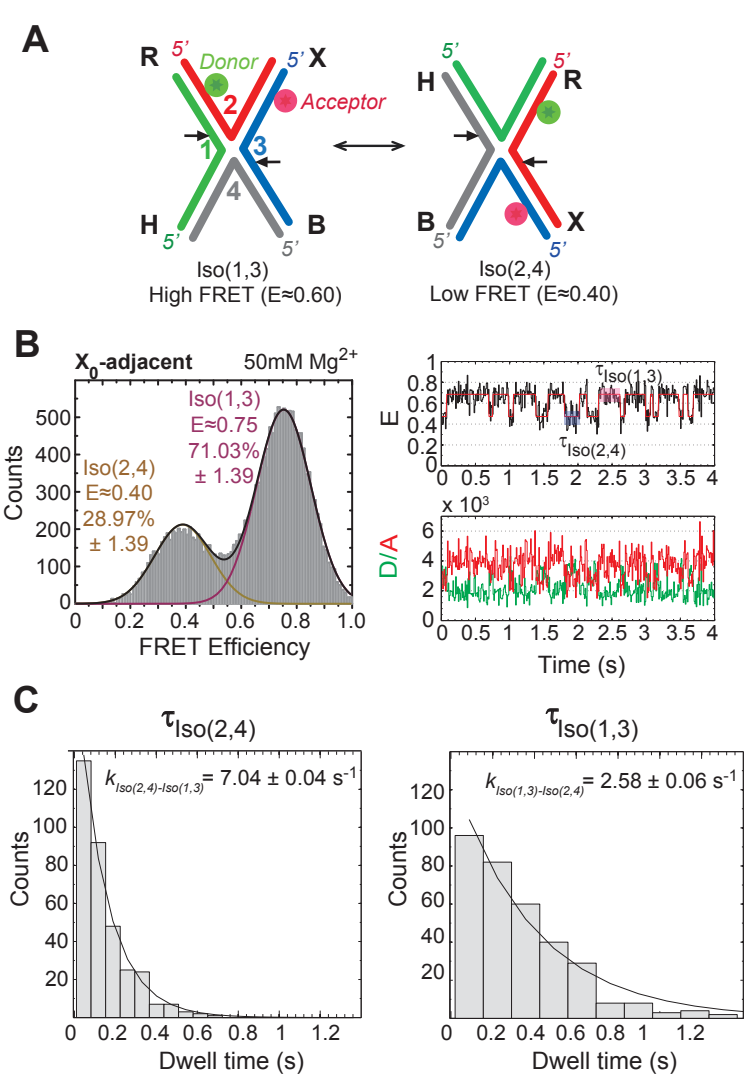


Figure 2 Conformer bias and Isomerization of the HJ .

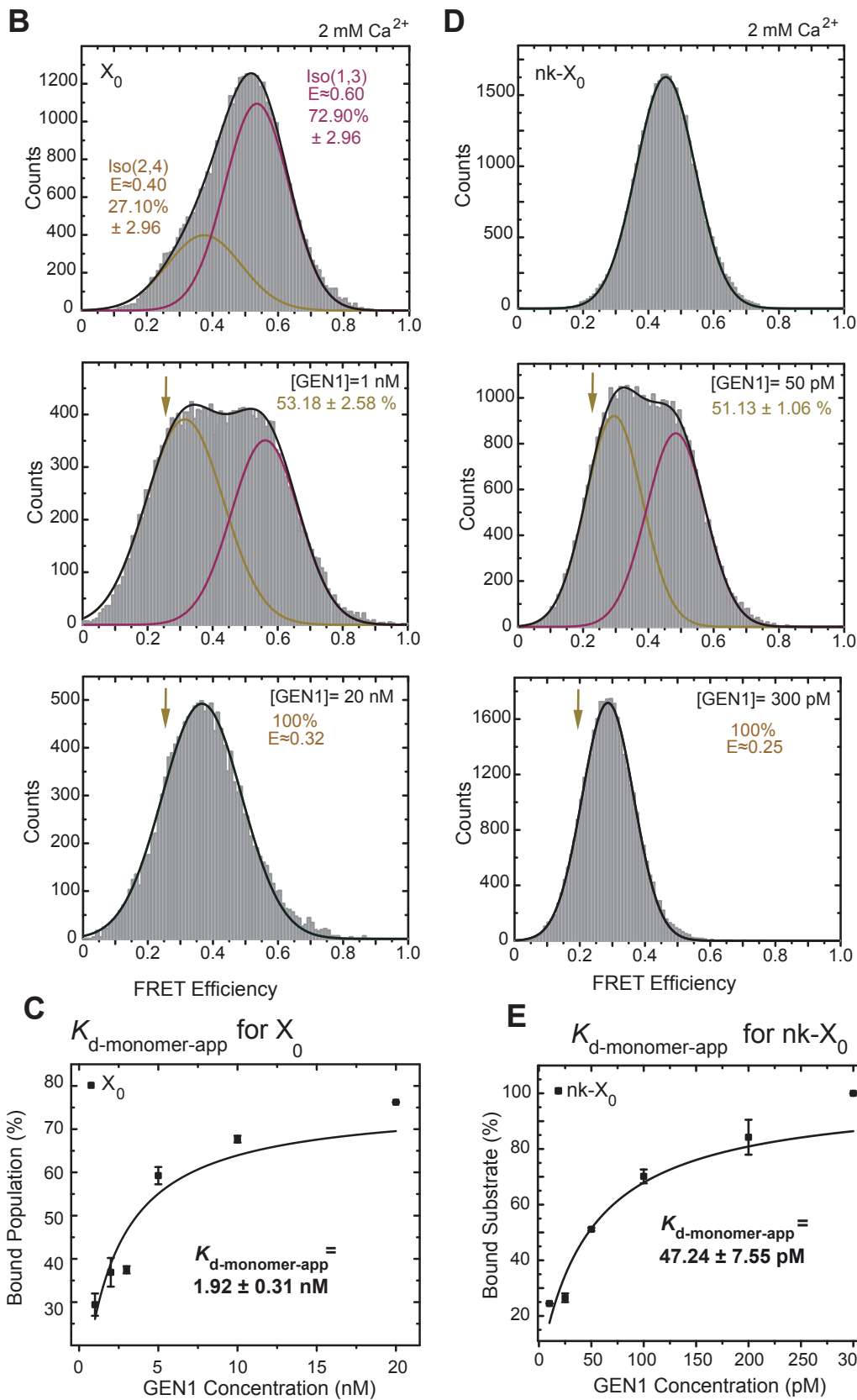
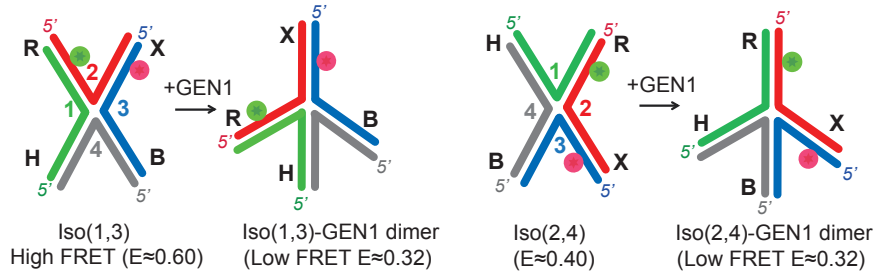


Figure 3 SMFRET demonstrates active distortion of the HJ by GEN1.

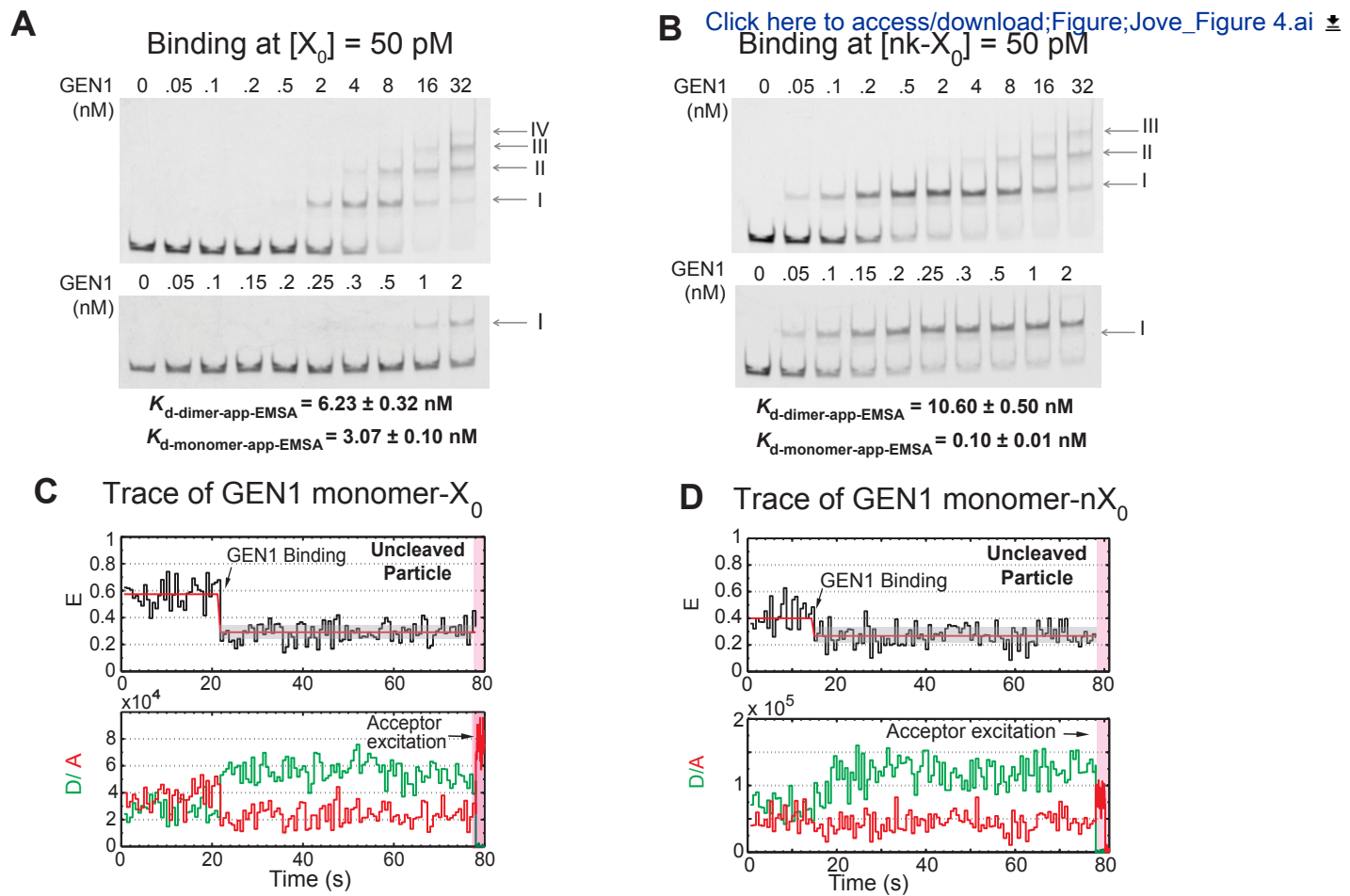


Figure 4 Stepwise binding of GEN1 monomer to the HJ.

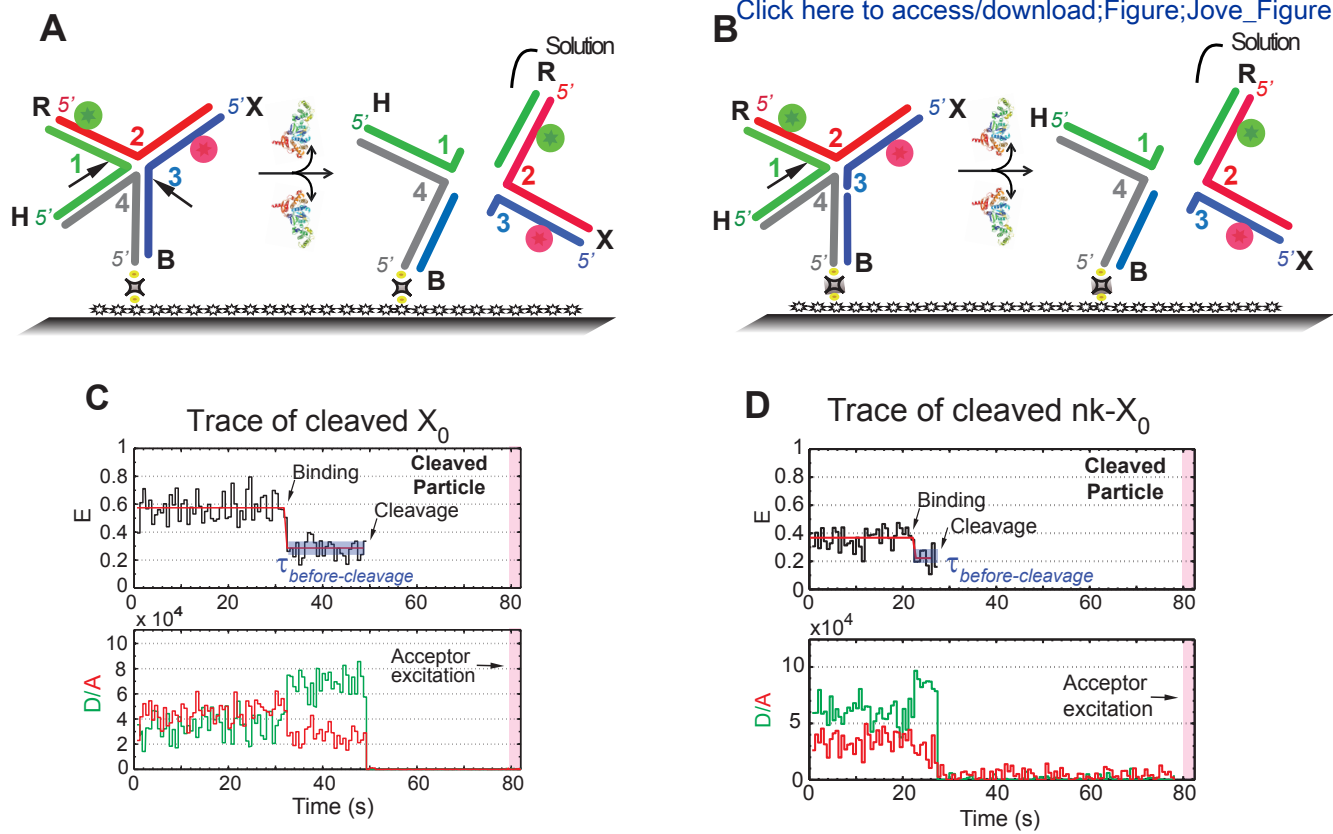


Figure 5 SMFRET resolution assay of the HJ.

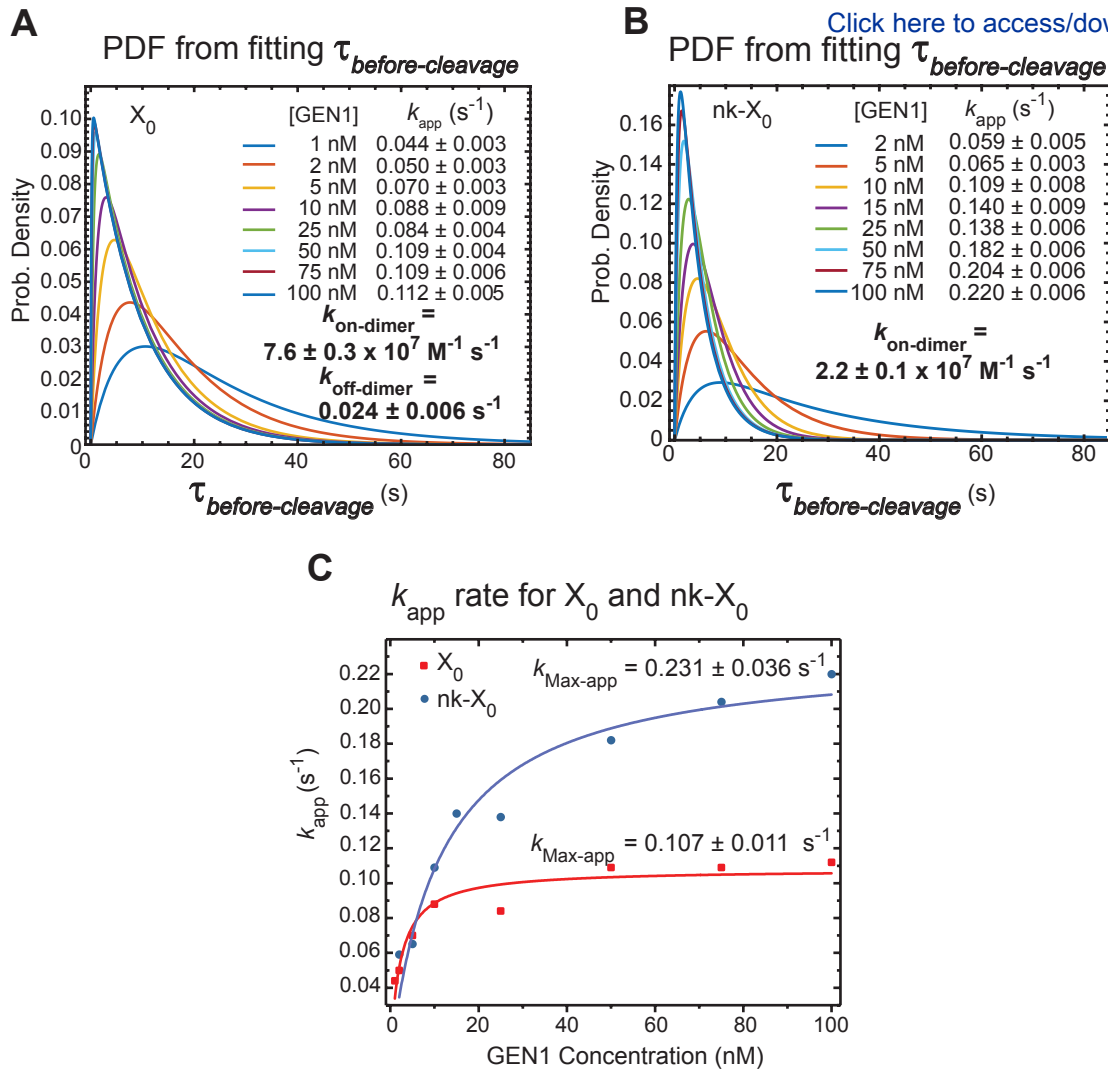


Figure 6 Kinetics of GEN1 dimerization on GEN1 monomer bound HJ.

Table 1.

Buffer
Binding buffer
Buffer A
Buffer B
Buffer C
Cleavage buffer
EMSA binding buffer
Imaging buffer (binding)
Imaging buffer (cleavage)
Lysis buffer
PCD storage buffer
storage buffer
TBE buffer
TE100 buffer
Tris-EDTA buffer

Compostion
40 mM Tris-HCl pH 7.5, 40 mM NaCl, 2 mM CaCl ₂ , 1 mM DTT, 0.1% BSA and 5% (v/v) glycerol
20 mM Tris-HCl pH 8.0, 1 mM DTT and 300 mM NaCl
20 mM Tris-HCl pH 8.0, 1 mM DTT and 100 mM NaCl
20 mM Tris-HCl pH 8.0 and 1 mM DTT
40 mM Tris-HCl pH 7.5, 40 mM NaCl, 2 mM MgCl ₂ , 1 mM DTT, 0.1% BSA and 5% (v/v) glycerol
40 mM Tris-HCl pH 7.5, 40 mM NaCl, 1 mM DTT, 2 mM CaCl ₂ , 0.1 mg/ml BSA, 5% (v/v) glycerol and 5 ng/μl Poly-dI-dC
40 μL (±)-6-Hydroxy-2,5,7,8-tetramethylchromane-2-carboxylic acid (4 μM), 60 μL PCA (6 nM), 60 μL PCD (60 nM) and 840 μL of Binding buffer
40 μL (±)-6-Hydroxy-2,5,7,8-tetramethylchromane-2-carboxylic acid (4 μM), 60 μL PCA (6 nM), 60 μL PCD (60 nM) and 840 μL of Cleavage buffer
20 mM Tris-HCl pH 8.0, 10 mM β-mercaptoethanol, 300 mM NaCl and 2 mM PMSF
100 mM Tris-HCl pH 7.5, 1 mM EDTA, 50 mM KCl and 50% glycerol
20 mM Tris-HCl pH 8.0, 1 mM DTT, 0.1 mM EDTA, 100 mM NaCl and 10% glycerol
89 mM Tris-HCl, 89 mM Boric acid and 2 mM EDTA
10 mM Tris.HCl pH 8.0 and 100 mM NaCl
50 mM Tris-HCl pH 8.0 and 1 mM EDTA pH 8.0

Table 2.

Oligo	Sequence
X ₀ -st1	ACGCTGCCGAATTCTACCAGTGCCTTGCTAGGACATCTTTGCCACCTGCAGGTTCACCC
X ₀ -st2	GGGTGAACCTGCAGGTGGG/iCy3/AAAGATGTCCATCTGTTGTAATCGTCAAGCTTTATGCCGT
X ₀ -st3	ACGGCATAAAGCTTGACGA/iAF647-dT/TACAACAGATCATGGAGCTGTCTAGAGGATCCGACTATCG
X ₀ -st4	5'BiotinCGATAGTCGGATCCTCTAGACAGCTCCATGTAGCAAGGCACTGGTAGAATTCGGCAGCGT
X₀-Adj	X₀-st1, X₀-st2, X₀-st3 & X₀-st4
X ₀ In_st2	GGGTGAACCTGCAGGTGGGCAAAGATGTCCATCTGTTGTAATCGTCAAGCTTTATGCCGT
X ₀ In_st4	5'BiotinCGATAGTCGGATCCTCTAGACAGCTCCATGTAGCAAGGCA/iCy3/TGGTAGAATTCGGCAGCGT
Nk-X₀	X₀-st1, X₀-st2, X₀-nk3a, X₀-nk3b & X₀-st4
X ₀ -nk3a	ACGGCATAAAGCTTGACGA/iAF647-dT/TACAACAGATC
X ₀ -nk3b	ATGGAGCTGTCTAGAGGATCCGACTATCG

Table 1.

Name	Company	Catalog Number
(±)-6-Hydroxy-2,5,7,8-tetramethylchromane-2-carboxylic acid (Trolox)	Sigma-Aldrich	238813
0.1 M sodium bicarbonate buffer	Fisher	144-55-8
10 % Novex Tris-Borate-EDTA gel	Thermo Fisher Scientific	EC6275BOX
100 X TIRF objective	Olympus	NAPO 1.49
3,4-dihydroxybenzoic acid (PCA)	Sigma-Aldrich	P5630
3-aminopropyltriethoxysilane (APTES)	Sigma-Aldrich	741442
6% Novex Tris-Borate-EDTA gel	Thermo Fisher Scientific	EC6265BOX
Adhesive sheet	Grace bio-labs	SA-S-1L
Benchtop refrigerated centrifuge	Eppendorf	Z605212
Biotin-PEG	Laysan Bio	Biotin-PEG-SVA 5000
Bovine Serum Albumin (BSA)	New England Biolabs	B9001S
Calcium Chloride Dihydrate	Sigma-Aldrich	31307
cation exchange column	GE healthcare	MonoS (4.6/100)
Cell disruptor	Constant Cell Disruption System	TS5/40/CE/GA
Coomassie Brilliant Blue	MP Biomedicals	808274
Cy3 emission filter	Chroma	HQ600/40M-25
Cy5/Alexa Fluor 647 emission filter	Chroma	HQ700/40M-25
Dichroic for DV2 filter cube	Photometrics	630dcxr-18x26
Dithiothreitol (DTT)	Thermo Scientific	R0861
Drill	Dremel	200-1/21
Electronic cutter	Copam	CP-2500
EMCCD camera	Hamamatsu	C9100-13
Epoxy glue	Devcon	14250
FPLC Akta purifier UPC 10	GE Healthcare	28406268
GelQuant.NET software	biochemlabsolutions.com	Version 1.8.2
GEN1 entry vector	Harvard plasmid repository	HSCD00399935
Glycerol	Sigma Life Science	G5516

green laser (emission 532 nm)	Coherent	Compass 315M-100
Heparin column	GE healthcare	HiTrap Heparin column
HEPES	BDH	BDH4162
Image splitter	Photometrics	Dualview (DV2)
Imidazole	Sigma-Aldrich	I2399
Inverted microscope	Olympus	IX81
Isopropyl- β -D-thiogalactoside (IPTG)	Goldbio.	12481C100
Laser scanner	GE healthcare	Typhoon Trio
LB Broth	Fisher Scientific	BP1426-500
Long pass 532nm filter	Semrock	LPD02-532RU-25
Magnesium Chloride	Sigma Life Science	M8266
mPEG	Laysan Bio	mPEG-SVA 5000
Neutravidin	Pierce	31000
Ni-NTA column	GE healthcare	HisTrap FF
NuPAGE 10% Bis-Tris gels	Novex Life technologies	NP0301BOX
NuPAGE 10% Bis-Tris Protein Gels	Thermo Fisher Scientific	NP0302PK2
Origin software	OriginLab Corporation	Version 8.5
Phenylmethylsulfonyl fluoride (PMSF)	Alexis Biochemicals	270-184-G025
Phosphate-buffered saline	GIBCO	14190
Polyethylene Tubing (I.D. 0.76 mm O.D. 1.22mm)	Fisher (Becton Dickinson)	427416
Protocatechuate 3,4-dioxygenase (3,4-PCD)	Sigma-Aldrich	P8279-25UN
Quad-band dichroic	Chroma Inc	Z405/488/532/640rpc
red laser (emission 640 nm)	Coherent	Cube 640 100C
Sodium Chloride	Fisher Chemical	S271
Sorvall RC-6 plus centrifuge	Thermo Fisher Scientific	46910
Spectrophotometer	Thermo Fisher Scientific	Nanodrop 2000
Syringe pump	Harvard Apparatus	70-3007
Teflon tweezers	Rubis	K35A
Tris Base	Promega	H5135
Ultracentrifuge	Beckman Coulter	Optima L-90K

Ultrafiltration membrane	Millipore	UFC90300
--------------------------	-----------	----------

ARTICLE AND VIDEO LICENSE AGREEMENT

Title of Article:	Single-molecule Förster resonance energy transfer methods for real time investigation of the resolution of the Holliday junction by Gap endonuclease I
Author(s):	Mohamed A. Sobhy, Amer Bralić, Vlad-Stefan Raducanu, Muhammad Tehseen, Yujing Ouyang, Masateru Takahashi, Fahad Rashid, Manal S. Zaher and Samir M. Hamdan

Item 1: The Author elects to have the Materials be made available (as described at <http://www.jove.com/publish>) via:

☐ Standard Access ☒ Open Access

Item 2: Please select one of the following items:

- ☒ The Author is **NOT** a United States government employee.
- ☐ The Author is a United States government employee and the Materials were prepared in the course of his or her duties as a United States government employee.
- ☐ The Author is a United States government employee but the Materials were NOT prepared in the course of his or her duties as a United States government employee.

ARTICLE AND VIDEO LICENSE AGREEMENT

1. **Defined Terms.** As used in this Article and Video License Agreement, the following terms shall have the following meanings: “**Agreement**” means this Article and Video License Agreement; “**Article**” means the article specified on the last page of this Agreement, including any associated materials such as texts, figures, tables, artwork, abstracts, or summaries contained therein; “**Author**” means the author who is a signatory to this Agreement; “**Collective Work**” means a work, such as a periodical issue, anthology or encyclopedia, in which the Materials in their entirety in unmodified form, along with a number of other contributions, constituting separate and independent works in themselves, are assembled into a collective whole; “**CRC License**” means the Creative Commons Attribution-Non Commercial-No Derivs 3.0 Unported Agreement, the terms and conditions of which can be found at: <http://creativecommons.org/licenses/by-nc-nd/3.0/legalcode>; “**Derivative Work**” means a work based upon the Materials or upon the Materials and other pre-existing works, such as a translation, musical arrangement, dramatization, fictionalization, motion picture version, sound recording, art reproduction, abridgment, condensation, or any other form in which the Materials may be recast, transformed, or adapted; “**Institution**” means the institution, listed on the last page of this Agreement, by which the Author was employed at the time of the creation of the Materials; “**JoVE**” means MyJoVE Corporation, a Massachusetts corporation and the publisher of The Journal of Visualized Experiments; “**Materials**” means the Article and / or the Video; “**Parties**” means the Author and JoVE; “**Video**” means any video(s) made by the Author, alone or in conjunction with any other parties, or by JoVE or its affiliates or agents, individually or in collaboration with the Author or any other parties, incorporating all or any portion

of the Article, and in which the Author may or may not appear.

2. **Background.** The Author, who is the author of the Article, in order to ensure the dissemination and protection of the Article, desires to have the JoVE publish the Article and create and transmit videos based on the Article. In furtherance of such goals, the Parties desire to memorialize in this Agreement the respective rights of each Party in and to the Article and the Video.

3. **Grant of Rights in Article.** In consideration of JoVE agreeing to publish the Article, the Author hereby grants to JoVE, subject to **Sections 4** and **7** below, the exclusive, royalty-free, perpetual (for the full term of copyright in the Article, including any extensions thereto) license (a) to publish, reproduce, distribute, display and store the Article in all forms, formats and media whether now known or hereafter developed (including without limitation in print, digital and electronic form) throughout the world, (b) to translate the Article into other languages, create adaptations, summaries or extracts of the Article or other Derivative Works (including, without limitation, the Video) or Collective Works based on all or any portion of the Article and exercise all of the rights set forth in (a) above in such translations, adaptations, summaries, extracts, Derivative Works or Collective Works and (c) to license others to do any or all of the above. The foregoing rights may be exercised in all media and formats, whether now known or hereafter devised, and include the right to make such modifications as are technically necessary to exercise the rights in other media and formats. If the “Open Access” box has been checked in **Item 1** above, JoVE and the Author hereby grant to the public all such rights in the Article as provided in, but subject to all limitations and requirements set forth in, the CRC License.

ARTICLE AND VIDEO LICENSE AGREEMENT

4. **Retention of Rights in Article.** Notwithstanding the exclusive license granted to JoVE in **Section 3** above, the Author shall, with respect to the Article, retain the non-exclusive right to use all or part of the Article for the non-commercial purpose of giving lectures, presentations or teaching classes, and to post a copy of the Article on the Institution's website or the Author's personal website, in each case provided that a link to the Article on the JoVE website is provided and notice of JoVE's copyright in the Article is included. All non-copyright intellectual property rights in and to the Article, such as patent rights, shall remain with the Author.

5. **Grant of Rights in Video – Standard Access.** This **Section 5** applies if the "Standard Access" box has been checked in **Item 1** above or if no box has been checked in **Item 1** above. In consideration of JoVE agreeing to produce, display or otherwise assist with the Video, the Author hereby acknowledges and agrees that, Subject to **Section 7** below, JoVE is and shall be the sole and exclusive owner of all rights of any nature, including, without limitation, all copyrights, in and to the Video. To the extent that, by law, the Author is deemed, now or at any time in the future, to have any rights of any nature in or to the Video, the Author hereby disclaims all such rights and transfers all such rights to JoVE.

6. **Grant of Rights in Video – Open Access.** This **Section 6** applies only if the "Open Access" box has been checked in **Item 1** above. In consideration of JoVE agreeing to produce, display or otherwise assist with the Video, the Author hereby grants to JoVE, subject to **Section 7** below, the exclusive, royalty-free, perpetual (for the full term of copyright in the Article, including any extensions thereto) license (a) to publish, reproduce, distribute, display and store the Video in all forms, formats and media whether now known or hereafter developed (including without limitation in print, digital and electronic form) throughout the world, (b) to translate the Video into other languages, create adaptations, summaries or extracts of the Video or other Derivative Works or Collective Works based on all or any portion of the Video and exercise all of the rights set forth in (a) above in such translations, adaptations, summaries, extracts, Derivative Works or Collective Works and (c) to license others to do any or all of the above. The foregoing rights may be exercised in all media and formats, whether now known or hereafter devised, and include the right to make such modifications as are technically necessary to exercise the rights in other media and formats. For any Video to which this **Section 6** is applicable, JoVE and the Author hereby grant to the public all such rights in the Video as provided in, but subject to all limitations and requirements set forth in, the CRC License.

7. **Government Employees.** If the Author is a United States government employee and the Article was prepared in the course of his or her duties as a United States government employee, as indicated in **Item 2** above, and any of the licenses or grants granted by the Author hereunder exceed the scope of the 17 U.S.C. 403, then the rights granted hereunder shall be limited to the maximum

rights permitted under such statute. In such case, all provisions contained herein that are not in conflict with such statute shall remain in full force and effect, and all provisions contained herein that do so conflict shall be deemed to be amended so as to provide to JoVE the maximum rights permissible within such statute.

8. **Protection of the Work.** The Author(s) authorize JoVE to take steps in the Author(s) name and on their behalf if JoVE believes some third party could be infringing or might infringe the copyright of either the Author's Article and/or Video.

9. **Likeness, Privacy, Personality.** The Author hereby grants JoVE the right to use the Author's name, voice, likeness, picture, photograph, image, biography and performance in any way, commercial or otherwise, in connection with the Materials and the sale, promotion and distribution thereof. The Author hereby waives any and all rights he or she may have, relating to his or her appearance in the Video or otherwise relating to the Materials, under all applicable privacy, likeness, personality or similar laws.

10. **Author Warranties.** The Author represents and warrants that the Article is original, that it has not been published, that the copyright interest is owned by the Author (or, if more than one author is listed at the beginning of this Agreement, by such authors collectively) and has not been assigned, licensed, or otherwise transferred to any other party. The Author represents and warrants that the author(s) listed at the top of this Agreement are the only authors of the Materials. If more than one author is listed at the top of this Agreement and if any such author has not entered into a separate Article and Video License Agreement with JoVE relating to the Materials, the Author represents and warrants that the Author has been authorized by each of the other such authors to execute this Agreement on his or her behalf and to bind him or her with respect to the terms of this Agreement as if each of them had been a party hereto as an Author. The Author warrants that the use, reproduction, distribution, public or private performance or display, and/or modification of all or any portion of the Materials does not and will not violate, infringe and/or misappropriate the patent, trademark, intellectual property or other rights of any third party. The Author represents and warrants that it has and will continue to comply with all government, institutional and other regulations, including, without limitation all institutional, laboratory, hospital, ethical, human and animal treatment, privacy, and all other rules, regulations, laws, procedures or guidelines, applicable to the Materials, and that all research involving human and animal subjects has been approved by the Author's relevant institutional review board.

11. **JoVE Discretion.** If the Author requests the assistance of JoVE in producing the Video in the Author's facility, the Author shall ensure that the presence of JoVE employees, agents or independent contractors is in accordance with the relevant regulations of the Author's institution. If more than one author is listed at the beginning of this Agreement, JoVE may, in its sole

ARTICLE AND VIDEO LICENSE AGREEMENT

discretion, elect not take any action with respect to the Article until such time as it has received complete, executed Article and Video License Agreements from each such author. JoVE reserves the right, in its absolute and sole discretion and without giving any reason therefore, to accept or decline any work submitted to JoVE. JoVE and its employees, agents and independent contractors shall have full, unfettered access to the facilities of the Author or of the Author's institution as necessary to make the Video, whether actually published or not. JoVE has sole discretion as to the method of making and publishing the Materials, including, without limitation, to all decisions regarding editing, lighting, filming, timing of publication, if any, length, quality, content and the like.

12. **Indemnification.** The Author agrees to indemnify JoVE and/or its successors and assigns from and against any and all claims, costs, and expenses, including attorney's fees, arising out of any breach of any warranty or other representations contained herein. The Author further agrees to indemnify and hold harmless JoVE from and against any and all claims, costs, and expenses, including attorney's fees, resulting from the breach by the Author of any representation or warranty contained herein or from allegations or instances of violation of intellectual property rights, damage to the Author's or the Author's institution's facilities, fraud, libel, defamation, research, equipment, experiments, property damage, personal injury, violations of institutional, laboratory, hospital, ethical, human and animal treatment, privacy or other rules, regulations, laws, procedures or guidelines, liabilities and other losses or damages related in any way to the submission of work to JoVE, making of videos by JoVE, or publication in JoVE or elsewhere by JoVE. The Author shall be responsible for, and shall hold JoVE harmless from, damages caused by lack of sterilization, lack of cleanliness or by contamination due to

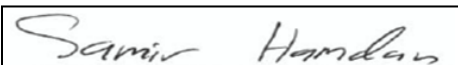
the making of a video by JoVE its employees, agents or independent contractors. All sterilization, cleanliness or decontamination procedures shall be solely the responsibility of the Author and shall be undertaken at the Author's expense. All indemnifications provided herein shall include JoVE's attorney's fees and costs related to said losses or damages. Such indemnification and holding harmless shall include such losses or damages incurred by, or in connection with, acts or omissions of JoVE, its employees, agents or independent contractors.

13. **Fees.** To cover the cost incurred for publication, JoVE must receive payment before production and publication of the Materials. Payment is due in 21 days of invoice. Should the Materials not be published due to an editorial or production decision, these funds will be returned to the Author. Withdrawal by the Author of any submitted Materials after final peer review approval will result in a US\$1,200 fee to cover pre-production expenses incurred by JoVE. If payment is not received by the completion of filming, production and publication of the Materials will be suspended until payment is received.

14. **Transfer, Governing Law.** This Agreement may be assigned by JoVE and shall inure to the benefits of any of JoVE's successors and assignees. This Agreement shall be governed and construed by the internal laws of the Commonwealth of Massachusetts without giving effect to any conflict of law provision thereunder. This Agreement may be executed in counterparts, each of which shall be deemed an original, but all of which together shall be deemed to be one and the same agreement. A signed copy of this Agreement delivered by facsimile, e-mail or other means of electronic transmission shall be deemed to have the same legal effect as delivery of an original signed copy of this Agreement.

A signed copy of this document must be sent with all new submissions. Only one Agreement is required per submission.

CORRESPONDING AUTHOR

Name:	Samir M. Hamdan	
Department:	Biological and environmental sciences and engineering division.	
Institution:	King Abdullah University of Science and Technology, Thuwal 23955, Saudi Arabia	
Title:	Associate Dean, Associate Professor of Biology	
Signature:		Date: 25 March 2019.

Please submit a **signed** and **dated** copy of this license by one of the following three methods:

1. Upload an electronic version on the JoVE submission site
2. Fax the document to +1.866.381.2236
3. Mail the document to JoVE / Attn: JoVE Editorial / 1 Alewife Center #200 / Cambridge, MA 02140

King Abdullah University of Science and Technology
Thuwal 23955-6900, Kingdom of Saudi Arabia

Samir M Hamdan
Associate Professor & Associate Dean
Biosciences Division

T +966 2 808 2384
M +966 54 470 0031



May 23, 2019

Editorial Board
JoVE

Dear Dr Bajaj,

We are thankful for your review of our manuscript (Sobhy et al. JoVE60045R1).

Please make the correspondence to Samir M. Hamdan (samir.hamdan@kaust.edu.sa) and Mohamed A. Sobhy (mohamed.sobhy@kaust.edu.sa).

The editorial comments were addressed and a summary of the implemented changes is presented below:

1. Please expand all abbreviations during the first-time use.

This change was applied in the summary.

2. Abstract should be between 150- 300 words. Presently this is less.

The abstract is now within limits and consists of 157 words

3. Protocol should not exceed 10 pages including headings and spacings. Presently it is more. Please combine some smaller steps and ensure that there are no more than 2-3 action per step.

The protocol now fits within the 10 pages limit. We made a separate table for the buffers.

4. Highlight should not exceed 2.75 pages including headings and spacings. Also, if a step is highlighted the heading or the subheadings associated with it should also be highlighted. Also, the entire sentence should be highlighted. Presently the highlight is more than the acceptable limit. Please adjust. Maybe highlights from step 1 can be removed?

The highlighted text is now 2.75 pages.

5. All notes will start from a new line. Please make this change throughout the manuscript.

The change was applied throughout the manuscript.

6. What is the desirable length in your case?

The desirable length is now mentioned "11 cm for the inlet and 25 cm for the outlet".

7. This is commercial. We cannot have commercial terms in our manuscript. Please use generic terms instead. Please include all commercial terms in the table of materials instead.

We now use the generic name "avidin" instead.

8. Expand please

3,4-PCD was expanded to Protocatechuate 3,4-dioxygenase.

9. Include the step number here

The statement was rephrased and we referred to the buffer composition in Table 3.

10. Refer to the table here.

We referred to the oligos in Table 2.

11. Please consider moving all the buffer compositions to a table instead. This table can be uploaded as a .xlsx file in your editorial manager. Please do not embed the table in the manuscript. The table can be then referred wherever applicable.

We made Table 3 for the buffers used in the manuscript and referred to that table wherever applicable.

12. We cannot have commercial terms in the manuscript. Please use generic terms instead.

We used the generic name “cation exchange column” instead of “MonoS”.

13. Please remove the white space. Please make the whole document as a continuous file.

The white space was removed.

14. Since there are so many buffers etc., I recommend putting the preparation step number as well wherever applicable throughout the manuscript. Imaging buffer (prepared in step...) Binding buffer (step...), etc

We referred to Table 3 for the buffers used throughout the manuscript.

15. Notes cannot be filmed so highlight is removed. Please convert to imperative tense and make it an action step if this needs filming.

We only included steps without notes now.

16. What is the desired concentration in this case?

We listed the used concentrations “1, 2, 5, 10, 25, 50, 75 & 100 nM”.

17. Please include these codes as supplemental file and refer it here.

The statements were rephrased to remove confusion. These are command lines to execute codes in Twotones which is an open source software.

18. Please explain what these are in the discussion section. Alternatively, provide references.

We provided the references.

19. Please combine table 1 and table 2 together. We cannot have two materials table.

Materials were combined in one table and arranged in alphabetic order.

20. Please make this a separate table and refer it in the text. Please include the legend here in the legend section.

We placed the table for the oligos in a separate excel file and referred to it in the text.

21. Please consider making a separate table for the compositions of the buffer used and place the legend here. The table can be referred wherever applicable.

We made a table for the buffers in a separate excel file and referred to it whenever applicable.

22. 38, 39 can be moved to the materials table instead.

References 38,39 were moved to the Materials table.

23. Please ensure that the references appear as the following: [Lastname, F.I., LastName, F.I., LastName, F.I. Article Title. Source. Volume (Issue), FirstPage – LastPage (YEAR).] For more than 6 authors, list only the first author then et al.
The references were formatted as requested.

24. The Figure must be cited appropriately in the Figure Legend, i.e. “This figure has been modified from [citation].”

The statement “This figure has been modified from reference 30.” was added to the legends of each of the figures 2 to 6.

Yours sincerely,



Samir M Hamdan

Associate Dean of Division of Biological and Environmental Sciences and Engineering
Associate Professor of Bioscience
Principal Investigator of the Laboratory of DNA Replication and Recombination
4700 King Abdullah University of Science and Technology
Thuwal 23955-6900, Kingdom of Saudi Arabia
Office: +966 2 808-2384 Cell: + 966 544700031 Email: samir.hamdan@kaust.edu.sa